Green Chemistry

PAPER

View Article Online
View Journal | View Issue

Cite this: *Green Chem.*, 2023, **25**, 1908

Seasonal dynamics in structural characteristics within bark stems of cultivated willow (*Salix* sp.) by NMR and time-gated Raman spectroscopy†

Jinze Dou, *[a] Martin Kögler,[b] Kavindra Kumar Kesari,[a] Leena Pitkänen[a] and Tapani Vuorinen[a]

The present study measures the seasonal dynamics of the chemical characteristics of pectin, hemicellulose, starch, protein, and soluble carbohydrates in the tissues of Scandinavian willow bark, which were examined during a complete annual cycle. Wet-chemical purification and non-destructive time-gated (TG) Raman spectroscopy were applied to illustrate the chemical characteristics as a response to the seasonal effect. Starch was found in a more complex linkage connection with hemicellulose and pectin in non-winter seasons, which is also supported by TG Raman spectroscopy. Interestingly, TG Raman spectroscopy also revealed that protein is more prominent in winter-harvested willow bark. The most striking seasonal effect investigated was in the structural characteristics of pectin. The pectin of winter-harvested willow bark has a larger proportion of the highly branched rhamnogalacturonan I (RG-I) domain compared to non-winter-harvested pectin. The study aims to build on this structural knowledge to provide seasonal-tailored enzymes and treat willow bark biologically so that sclerenchyma fibre bundles can be isolated. We demonstrate here for the first time that a combination of non-destructive TG Raman and wet-chemical purification identification methods provides more knowledge about the compositional changes throughout the seasonal variation of compounds in willow bark. The correlation between the seasonal dynamics and the structure of pectin from willow bark is discussed for the first time, which provides the essential knowledge required for optimizing the microbial consortium in valorizing willow bark that can possibly be harvested from multiple seasons.

Received 24th November 2022,
Accepted 19th January 2023

DOI: 10.1039/d2gc04476e

rsc.li/greenchem

Introduction

In the production of the pulp and paper industry, for example in mechanical pulp mills, bark represents roughly 10 wt% of tree logs.[1] Apart from the major constituents of wood (cellulose, hemicellulose, and lignin), the bark contains a significant number of compounds such as pectin, starch, and structural proteins.[2] The presence of high amounts of pectin and proanthocyanidin-enriched extractives in the bark may consume chemicals used in cooking and bleaching. Thus, they are considered as the least desirable fractions to be chemically consumed in a typical pulp and paper mill. Traditionally, the first step in pulp, paper, and timber production has been bark removal. Biological pretreatment[3] has been suggested as an ideal method so that the pretreated-wood can be more effectively chemically cooked to produce pulp fibers. In certain fast-growing trees (like willow,[4,5] eucalyptus,[6] and poplar[7]), lignified sclerenchyma fiber bundles are organized in a continuous distribution and are surrounded by non-lignified tissue (mostly pectin).

A tailor-made enzyme (pectinase and hemicellulase) consortium, which has been built up upon the structural characteristics of the substrate, succeeded in segregating sclerenchyma fiber bundles from willow bark.[4] The bark is a very complex tissue with many layers and seasonal/annual variations in biosynthesis, which is related to the formation of different tissues and cell types. One of the major obstacles in optimizing this "tailor-made enzyme consortium based on the structural features of the substrate" strategy[4] is simply the lack of a holistic approach to understanding the seasonal effects on structural features of major constituents in the bark cell walls, namely pectin and hemicellulose. Pectinases and hemicellulases could be tailored more precisely to liberate the sclerenchyma fiber bundle from the wood bark. For example, pectin synthesis is related to cell wall biosynthesis[8,9] and heat stress.[10] Although structural features of pectin have been reported to be

[a]*Department of Bioproducts and Biosystems, Aalto University, 02150 Espoo, Finland. E-mail: jinze.dou@aalto.fi; Tel: +358 413115001*
[b]*VTT Technical Research Centre of Finland, 90570 Oulu, Finland*
† Electronic supplementary information (ESI) available. See DOI: https://doi.org/10.1039/d2gc04476e

related to the seasonal cycle of fruit plants (such as citrus[11]) and wood (such as poplar[12] and spruce[13]), this seasonal variation has very rarely been reported in wood bark.

Understanding the chemical structure of pectin and hemicellulose is essential for designing a customized biological treatment to smartly recover the sclerenchyma fiber bundles from wood bark. Pectin consists mainly of a "smooth" region of homogalacturonan (HG) and rhamnogalacturonan I (RG-I) that are substituted at O-4 through side chains of arabinan, galactan, and arabinogalactan. The skeleton of RG-I has been considered the "hairy region" of pectin, which consists of 1,4-linked galacturonic acid (GalA) and 1,2-linked rhamnose units. Compared with strong mineral acids, extraction with citric acid is known to retain the pectin structure to its maximum extent.[14] Additionally, hemicelluloses, the second most abundant group of polysaccharides, play an important role in strengthening the structural properties of the cell wall. Also, glucuronoxylan and xylan are the most prominent hemicelluloses.[15] Glucuronoxylan, as the primary hemicellulose in hardwood, contains xylose and glucuronic acid as the main constituents. It is characterized by a linear β-(1,4)-linked β-D-xylopyranosyl units and substituted by 4-*O*-methyl-D-glucuronic acid (–MG) and acetyl groups. Alkaline extraction[16] and peracetic acid delignification followed by DMSO extraction[17] are conventional methods to extract hemicellulose from wood. However, hemicellulose extraction from tree bark has seldom been reported.

Raman spectroscopy is recognized as a non-deconstructive technique for the characterization of complex biochemical structures, and in comparison to other vibrational spectroscopic methods, such as near-infrared spectroscopy, there is very little interference from water. However, one limiting factor is the strong fluorescence background that may be superimposed on the weak signal from Raman scattering of the sample when using traditional continuous wave (CW) excitation Raman.[18] In particular, lignin-containing compounds often suffer from high fluorescence. An advanced novel approach to overcome this is time-gated (TG) Raman spectroscopy that makes use of a pico-second pulsed laser synchronized with the detector to be able to "gate-out" the disturbing background signals, such as fluorescence, before they have a chance to spoil the actual Raman signal of the sample.

Herein, we followed classical protocols to extract and further identify differences in structural features of multiple fractions (*i.e.* extracts, pectin, and hemicellulose) from willow bark that was harvested at five intervals throughout one calendar year. Newer pretreatments have been developed to recover the hemicellulose fraction, particularly from bark. Furthermore, time-gated Raman spectroscopy was implemented as a non-destructive novel technique to reveal the structural profile from the original form of willow bark with a drastically reduced fluorescence background. Both destructive and non-destructive techniques were employed to explore the correlation between the chemical composition of polysaccharides (particularly of pectin, hemicellulose, starch, and pectin) and seasonal variations.

Material and methods

Materials and chemicals

Willow hybrid Klara was harvested at five intervals (Fig. 1) throughout the year 2020 from Carbons Finland Oy (Kouvola, Finland). The willow bark was manually peeled and Wiley-

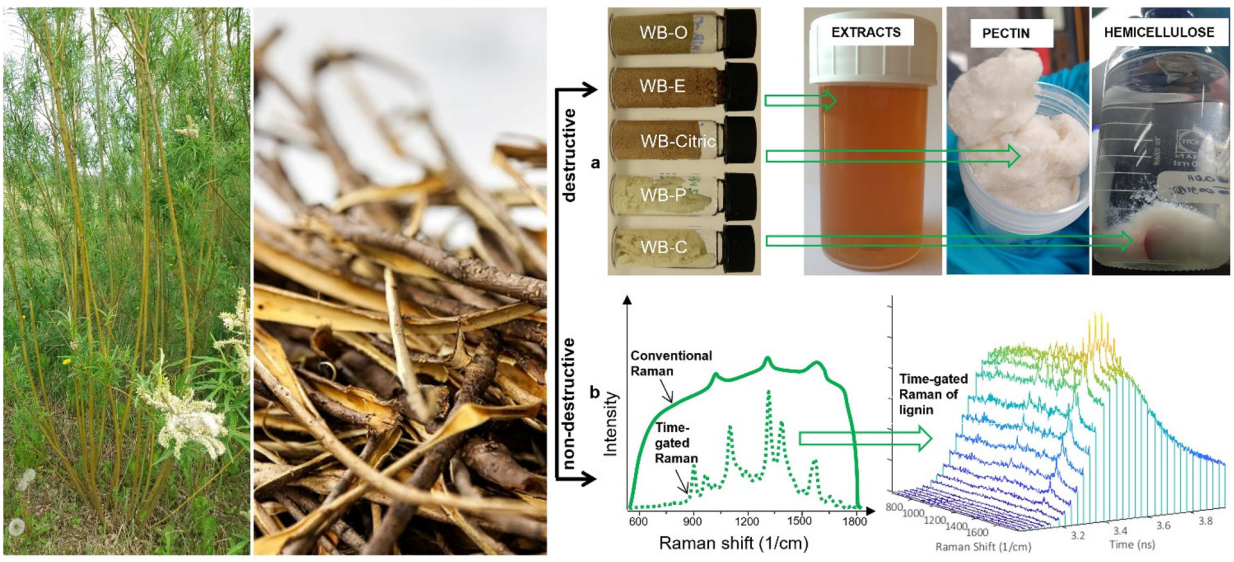

Fig. 1 Analyzed willow bark biomass and implemented characterization techniques. (a) Illustration of multiple steps of the experimental flow for preparing water-soluble extracts, pectin, and hemicellulose (also cellulose) from willow bark that was harvested at five different seasons during a complete annual cycle: 02-17 (17th February); 04-23 (23rd April); 07-13 (13th July); 09-23 (23rd September); 12-04 (4th December). (b) Raman spectroscopy is applied as a non-destructive technique for acquiring the chemical profile of the native form of willow bark.

milled (<1 mm mesh) and stored at −20 °C before further use. Acetone, arabinose, citric acid, dichloromethane, dimethyl sulfoxide (DMSO), DMSO-d_6, ethanol, ferulic acid, formic acid, fructose, galactose, glucose, hydrochloric acid, mannose, methanol, pectin from citrus peel (galacturonic acid > 74%), pepsin, peracetic acid, pyridine-d_5, rhamnose, sodium hydroxide, starch (practical grade from corn), and xylose were purchased from Sigma-Aldrich, Finland. Kraft lignin (BiPiva™ 100) was purchased from UPM-Kymmene Oyj.

Experimental flow

The milled original form (O) of willow bark was extracted under a Soxhlet unit (Electromantle: ColeParmer Extractors: Lenz). Three different solvents (*i.e.*, water, dichloromethane, and acetone) were utilized for 4 h/solvent to remove both lipophilic and hydrophilic extracts. Extracts only soluble in water were recovered using a freeze-dryer and the lyophilized water-soluble extracts were kept in a desiccator for further characterization. The experimental flow comprised two additional major steps: pectin recovery using citric acid and hemicellulose recovery, as presented in Fig. 1.

Pectin extraction using citric acid treatment. Extract-free solid residues (E) were extracted with prepared citric acid (1 : 30, w/v, pH 2) for 60 min at a temperature of 90 °C to chelate pectin polysaccharides. The soluble liquid fractions were recovered through a membrane (diameter size of 15–20 μm) and the citric-acid-treated solid residue (Citric) was preserved for further steps (Fig. 1). Ethanol was added to the filtered liquid with a final ethanol concentration of 75 v/v% and the liquid mixture was stored in cold conditions (+5 °C) for pectin precipitation. Centrifugation (8000 rpm, Eppendorf 5804R) and freeze drying were implemented to obtain lyophilized crude citric acid pectin (CAP). The CAP was further purified using dialysis membranes (Spectra/Por, MWCO 6–8 kDa, 96 h) to remove small molecular weight compounds. Finally, the dialyzed citric acid pectin (DCAP) was further centrifuged and freeze-dried for structural characterization.

Hemicellulose extraction. The citric-acid-treated solid residue (Citric) was mixed with 1% pepsin in 0.1 M HCl (liquid-to-solid ratio of 25 : 1) at 37 °C for 16 h in an incubation shaker at a speed of 300 rpm (CERTOMAT, Sartorius Biotech Inc.). The protein-free solid residue was further rinsed with hot water until the washing liquid became neutral. Most of the tannin-type compounds were removed with further treatment using 0.1 M NaOH (1/50, w/v) under nitrogen flow at 100 °C for 1 h and the solid residue was washed with water. Approximately 5 g of 0.1 M NaOH treated solid residue was processed further with delignification (1/30, w/v) using 10% peracetic acid at 85 °C at pH 4.0 for 1 h.[17] The solid residues of holocellulose (P) were further extracted twice with DMSO (1/30, w/v) at 50–60 °C for 12 h. The united DMSO extracts (pH 3) were precipitated in 1 L of EtOH : MeOH mixture (7/3, v/v), and the hemicellulose was recovered after centrifugation. Once the residual solvent was eliminated from the hemicellulose under a fume hood, freeze-drying was introduced to obtain the lyophilized hemicellulose (H). The solid residue (C) after DMSO extraction was rich in cellulose and collected for further analysis.

Analytics

Several chromatographic (HPAEC-PAD, HPLC, and SEC) and spectroscopic (Raman and NMR) techniques were employed for chemical characterization. Viscosity measurement was implemented only for the purified cellulose.

Chromatographic techniques

Chemical compositional analysis by PAD. The chemical composition of the willow bark and its associated biomass residues (Fig. 1) was determined according to NREL/TP-510-4261831. Quantitation of the hydrolyzed monosaccharide was determined using a high-performance anion-exchange chromatography-pulsed amperometric detector (HPAEC-PAD, Dionex 3000 ICS), equipped with a CarboPac PA20 column (Sunnyvale, CA, USA) for carbohydrates. The eluent (pure water) was set at a flow rate of 0.38 ml min^{-1} at room temperature.

High-performance liquid chromatography (HPLC). The determination of galacturonic acid by acid hydrolysis is known to lead to the degradation of galacturonic acid.[4] A recovery coefficient of 59.2% was considered and applied for quantification of galacturonic acid using HPLC (Dionex Ultimate 3000) equipped with a refractive index detector and column module of phenomenex Rezex ROA-Organic Acid H+ (8 μm, 300 × 7.8 mm, Thermo Scientific, USA). The eluent (0.0025 M H_2SO_4) was set at a 0.5 ml min^{-1} flow rate at 55 °C.

Size-exclusion chromatography (SEC) (molar mass determination for pectin, hemicellulose, and cellulose) and viscosity measurement (for cellulose). SEC experiments for the analysis of hemicellulose and pectin were carried out with an Agilent 1260 Infinity II Multi-Detector GPC/SEC System including a refractive index detector. Three Waters 7.8 mm × 300 mm Ultrahydrogel columns (500 Å, 250 Å, and 120 Å) with a 6 mm × 40 mm Ultrahydrogel guard column were used with a flow rate of 0.5 ml min^{-1} to separate the pectin using 0.1 M NaCl as an eluent. Two Agilent PLgel MIXED-B columns (7.5 mm × 300 mm) with a PLgel guard column (7.5 mm × 50 mm) were used with a flow rate of 0.5 ml min^{-1} for separation of hemicelluloses using DMSO as the eluent. The injection volume was 100 μl in both cases. For molar mass determination, the columns were calibrated using narrow dispersity pullulan standards. The cellulose-rich samples were dissolved in 0.9% LiCl in DMAc after a solvent exchange procedure with water, acetone, and DMAc.[19] Dionex Ultimate 3000 HPLC module coupled with Shodex DRI (RI-101) and Viscotek/Malvern SEC/MALS 20 multi-angle light-scattering (MALS) detectors were used. The Agilent PLgel MIXED-A (×4) columns were implemented with a flow rate of 0.75 ml min^{-1}. A narrow dispersity polystyrene sample (M_w = 96 000 g mol^{-1}, $Đ$ = 1.04) (dissolved in the same solvent of LiCl/DMAc) was used to determine the constants for both MALS and DRI detectors. A $\partial n/\partial c$ value of 0.136 ml g^{-1} was used for cellulose in 0.9% LiCl/DMAc. The viscosities of the cellulose were also determined

with cupriethylenediamine (CED) according to the standard SCAN-CM 15:99.

Spectroscopic techniques

Nuclear magnetic resonance (NMR) spectroscopy was applied for analyses of the linkage structures of pectin and hemicellulose, respectively. Spectra were processed using a Topspin 4.0 (Bruker) and colorized using Adobe Illustrator 2023 (Adobe Inc.). The detailed experimental parameters are summarized below.

^{1}H and heteronuclear single quantum coherence (HSQC) for pectin. Measurements were conducted using a 400 MHz Bruker Avance III spectrometer. 3-(Trimethylsilyl)propionic-2,2,3,3-d_4 acid sodium salt (TSP-d_4) (δ_C/δ_H, 0/0 ppm) was used as the internal reference for chemical shift calibration and ^{1}H NMR quantitation. ^{1}H NMR spectroscopy was implemented to calculate the degree of methylation (DM) and acetylation (DA) of the pectin according to the literature.[20] Spectra were measured with a relaxation delay of 5 s with 170 scans. 2D HSQC was used to correlate the proton and carbon shifts, and their measurements were conducted using a relaxation delay of 2 s with 96 scans.

HSQC for hemicellulose. 2D ^{1}H–^{13}C HSQC measurement was conducted using a 400 MHz Bruker Avance III spectrometer.[4] DMSO-d_6/pyridine-d_5 (v/v, 4/1) was adopted as a deuterated solvent for chemical shift calibration. 2D HSQC NMR spectra were obtained with a relaxation delay of 1 s and 195 scans.

Time-gated Raman spectroscopy. Willow bark samples (O) were analyzed using a wavelength-calibrated commercial time-gated Raman spectrometer (PicoRaman from Timegate Instruments Oy, Oulu, Finland), with a reduced-power 10 mW pulsed laser at λ_{exc} = 532 nm excitation, 100 kHz repetition rate and 100 ps pulse length. The temperature-stabilized CMOS-SPAD array (single photon counting 8 × 768 pixels) detector at a spectral resolution of 5 cm^{-1} and temporal resolution of 100 ps was connected to a conventional non-immersion Raman probe with quartz window material (BWTek, BAC102, Metrohm, Herisau, Switzerland) and a working distance of 5.4 mm. To avoid sample burning, samples were wetted with ultra-pure water and a rotational sample table with a constant speed of approximately 80 rpm was used. The measurement time for each sample with time-gated Raman spectroscopy (TG-RS) was set to 3 times 60 s including repetitions to achieve an appropriate signal without sample evaporation. Raman measurements were set to cover the range of interest in the fingerprint region from 200 to 2000 cm^{-1}. Continuous wave (CW) Raman (Renishaw inVia Qontor, Wotton-under-Edge, UK) was also implemented for recording a single spectrum of authentic compounds using continuous laser excitation at λ_{exc} = 532 nm. Raman spectra were analyzed with OriginPro (Version 2022b, OriginLab Corporation, Northampton, MA, USA). Spectral data were intensity normalized within the interval from 0 to 1, smoothed with a 5-point Savitzky–Golay filter of 2nd polynomial order, and for better presentation plotted with an offset.

Results and discussion

Mass balance and seasonal effect on recovered extracts and cellulose

The chemical composition of willow bark is measured as hexoses after acid hydrolysis of di- and oligosaccharides. In general, the seasonal dynamics of the hydrolyzed monosaccharides were significantly pronounced in the investigated samples, as shown in Fig. 2. The overall carbohydrate content reached its maximum in summer-season-harvested willow bark (WB) (*i.e.* 07-13), which is roughly 20%, 15%, and 10% higher than the winter-harvested (*i.e.* 02-17 and 12-04), spring-harvested (04-24), and late-autumn-harvested WB (09-23), respectively. However the recovered cellulose (with a repeating unit of β-glucose) content (Table S1†) differed from the overall trend of the carbohydrates (Fig. 2a), suggesting that the determined glucose (Fig. 2b) was possibly partly derived from starch. The exact conversion mechanism between starch and sugar is not within the scope of this study. Glucose was the main monosaccharide found in all samples, whereas xylose and mannose were the dominant non-cellulosic sugars besides pectin-characteristic monosaccharides. A comparison of the xylose/mannose ratio indicates that xylan was the main hemicellulose component in all investigated willow bark. Pectin characteristics (arabinose, rhamnose, galactose, galacturonic acid) were equally present in all the bark (Fig. 2b). The acid-insoluble "lignin" content of WB (O) (Fig. 2a) was roughly 15–20% higher than that of 0.1 M NaOH treated solid residues (N) (Table S1 and Fig. S1†), suggesting the overestimation of the acid-insoluble "lignin" was probably caused by the heterogenous chemicals that originated from the extractives, pectin, protein, and proanthocyanidins. Overall, the seasonal variation in the carbohydrate content of willow bark is clear and suggests that the bark tissues have a potential physiological role in synthesizing carbohydrates for over-wintering purposes. A similar observation about seasonal dynamics has previously been reported for the woody stems of *Cornus sericea* L.[21] and *Salix caprea* L.[22] as well as oak and beech,[23] however, it is seldom reported for the bark.

Similar seasonal variation also seems to be pronounced when looking at the sucrose and raffinose from the extractive composition, which was more abundantly present in water extract samples that are harvested during winter. A similar observation has been reported for the willow bark of other *Salix* hybrids (Tordis, Schwerenee, Winter, and Tora).[24] Raffinose, known as a cryoprotectant oligosaccharide, has a high response to the cold hardening of *Salix*.[21,25]

Seasonal effect on pectin

To liberate the acidic polysaccharide pectin from willow bark, pH 2 citric acid was introduced as a chelating agent, and samples were correspondingly named CA-P. The crude pectin yield of winter-harvested samples (12-04 and 02-17) was slightly smaller than that of quantities purified from other seasons, such as early spring (04-23), the middle of summer (07-13), and the middle of autumn (09-23) (Table 1). In particu-

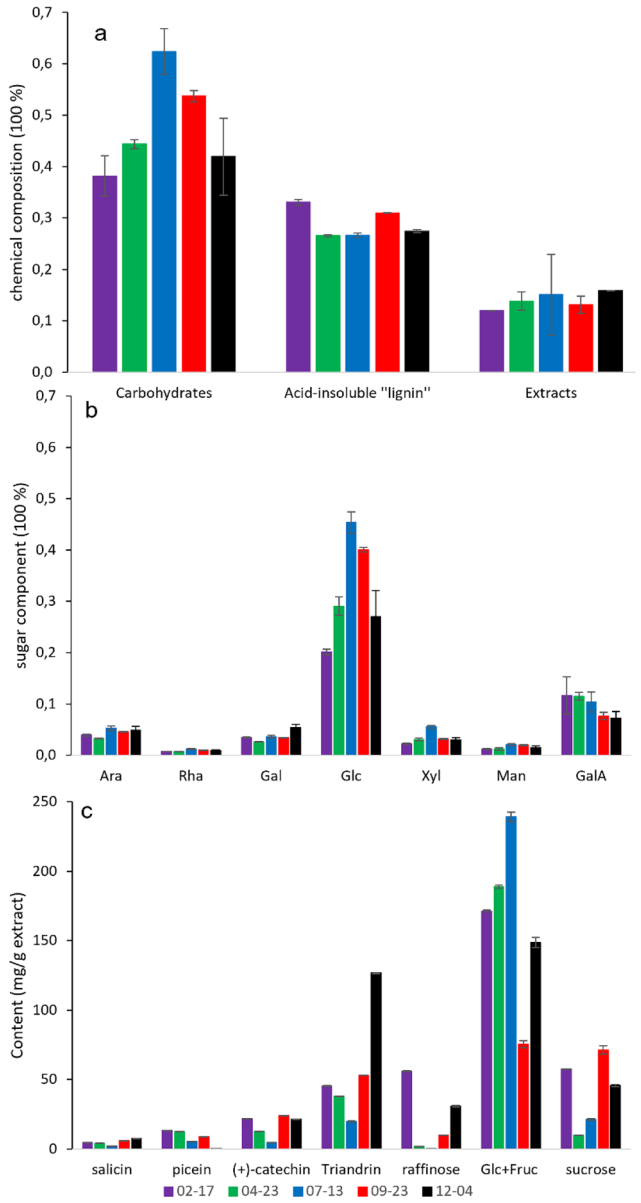

Fig. 2 Chemical compositional analysis of the original form (O) of willow bark (02-17; 04-23; 07-13; 09-23; 12-04). (a) An overall chemical composition (% of the accepted dry mass) after acid hydrolysis of di- and oligosaccharides. (b) Carbohydrate composition (% of anhydro sugars in the monosaccharide) after acid hydrolysis of di- and oligosaccharides. (c) Chemical composition of the water-soluble extracts (without hydrolysis). For a detailed chemical profile of the sample after each pretreatment of citric acid extraction plus 0.1 M NaOH (N), peracetic acid delignification (P), recovered hemicelluloses (H), and the recovered cellulose (C), see Fig. S1.† Abbreviations: arabinose (Ara), rhamnose (Rha), galactose (Gal), glucose (Glc), xylose (Xyl), mannose (Man), galacturonic acid (GalA), fructose (Fruc).

lar, the gravimetric yield of purified pectin has an almost equal presence in all seasons of willow bark. The dialysis treatment removed almost half to two-thirds of the small molecular weight fractions from crude pectin. Although dialysis of CA-P had a minimal effect on neutral monosaccharide composition (Table 1 and Fig. S2†), the treatment resulted in a roughly two to three-fold increase in GalA in all pectin samples. The relative amount of glucose in pectin harvested in winter was much smaller than in other seasons, suggesting that glucose may be derived in part from starch, and the mobilization of starch-to-sugar is well known as a self-regulatory mechanism for responding to cold acclimation. This starch breakdown mechanism during temperature stress[26] has also been reported for tree species of willow[22] and poplar.[27] The ratio of Rha/GalA is generally low for pectin that is recovered from all samples, indicating there are higher HG fragments in the bark that are harvested from all seasons. This observation is also supported by the significant presence of GalA in recovered pectin. Interestingly, the (Gal + Ara)/Rha ratio was highest in early winter (10.6, 12-04) and slowly dropped until midsummer (5.9, 07-13), indicating that pectin harvested in winter had roughly twice as many branched RG-I domains as summer-harvested pectin (07-13). The degree of methylation (DM) and acetylation (DA), and M_w of recovered pectin from late winter (02-17) were the lowest among all pectin samples (Table 1).

Solution-state 2D HSQC NMR (Fig. 3) revealed typical inter-unit linkages of pectin, and its spectra were assigned based on the literature[4,28,29] and authentic starch (Fig. S3†). Three clear signals at δ_C/δ_H of 56.0/3.81, 23.4/2.09, and 19.5/1.26 ppm indicate the presence of methyl groups of 1,4-α-D-GalpA (OMe), 1,4-α-D-GalpA (OAc), and rhamnose, respectively. The non-anomeric methylene of GalA (δ_C/δ_H of 71.5/3.92, 71.5/4.01, 73.5/5.09, and 83.6/4.29 ppm) was also confirmed. Interestingly, strong starch (1,4-α-D-Glc*p*) signals were identified mostly in non-winter-harvested pectin at C1/H1 (102.8/5.40), C2/H2 (74.8/3.64), C3/H3 (76.4/3.96), C4/H4 (79.8/3.67), C5/H5 (74.35/3.83), and C6/H6 (63.9/3.83 ppm), confirming that starch linked with pectin can possibly act as energy storage in response to the chilling season. Specific non-anomeric and anomeric methine signals revealed the presence of arabinofuranosyl groups (terminal and 1,5-, 2,5-, and 2,3,5-linked) from the pectin that are recovered from all seasons. However, an almost negligible amount of galactopyranosyl groups was detected from the pectin of non-winter-harvested seasons (04-23, 07-13, and 09-23) in comparison to the pectin recovered from winter seasons (12-04 and 02-17). Overall, the temperature affects the biosynthesis of pectin. Starch was abundantly linked with the pectin that is harvested during non-winter seasons (04-23, 07-13, and 09-23). The presence of high amounts of galactose indicated that the pectin recovered from winter-season WB was more highly branched than in other seasons, which is also in line with the value of (Gal + Ara)/Rha (Table 1).

Pectin is chemically heterogenous from winter-harvested pectin (02-17 and 12-04) to non-winter-harvested pectin (04-23, 07-13, and 09-23) (Table 1). Therefore the enzyme consortium[4] also needs to be tailored based on the substrate structure and specific characteristics of the enzymes. For pectin, the ratio and composition of the HG and RG-I regions affect its degradation by pectinases. The pectin of winter-harvested WB (*i.e.* 12-04 and 02-17) showed a high proportion of highly branched RG-I and was rich in non-branched galactan sidechains, indicating the necessity of selecting galactanase as part of the

Table 1 Yield, weight-average molecular weight (M_w), dispersity (M_w/M_n), and chemical composition of ethanol-precipitated pectin from treatments with aqueous citric acid before (CA-P) and after (DCA-P) dialysis from five different samples: 02-17; 04-23; 07-13; 09-23; 12-04

	02-17-CA-P	02-17-DCA-P	04-23-CA-P	04-23-DCA-P	07-13-CA-P	07-13-DCA-P	09-23-CA-P	09-23-DCA-P	12-04-CA-P	12-04-DCA-P
Pectin yield (% WB)	3.3	2.1	4.0	1.5	3.9	1.7	4.3	1.5	2.9	1.3
M_w (kDa)		135		300		237		234		207
M_w/M_n		1.4		5.3		5.2		5.4		4.6
Monosaccharides (mg g^{-1})										
Ara	80 (1)	49 (0)	76 (2)	115 (0)	67 (2)	104 (0)	52 (1)	83 (0)	95 (2)	122 (0)
Rha	23 (0)	16 (0)	24 (1)	29 (0)	21 (1)	29 (0)	16 (0)	23 (0)	26 (1)	29 (0)
Gal	126 (1)	77 (1)	108 (3)	107 (0)	52 (1)	75 (0)	59 (1)	74 (0)	191 (4)	205 (0)
Glc	47 (2)	29 (1)	352 (10)	202 (0)	280 (8)	168 (0)	687 (12)	412 (3)	22 (0)	18 (1)
Xyl	4 (6)	2 (3)	3 (0)	4 (0)	4 (0)	3 (0)	1 (1)	3 (0)	3 (0)	4 (1)
Man	4 (6)	2 (3)	5 (0)	4 (1)	3 (0)	1 (1)	1 (2)	6 (0)	5 (0)	7 (0)
GalA	178 (0)	450 (0)	138 (0)	446 (0)	138 (0)	340 (0)	90 (0)	307 (0)	168 (0)	446 (0)
Overall	463	624	707	907	564	721	906	908	511	832
Molar composition										
Rha/GalA	0.2 (0.002)	0.0 (0.001)	0.2 (0.009)	0.1 (0)	0.2 (0.006)	0.1 (0)	0.2 (0.005)	0.1 (0)	0.2 (0.005)	0.1 (0.001)
(Gal + Ara)/Rha	8.9 (0.03)	7.7 (0.1)	7.5 (0.1)	7.7 (0.02)	5.9 (0.05)	6.2 (0.02)	6.9 (0.1)	6.8 (0.05)	10.6 (0.1)	11.0 (0.2)
HG (mol%)	29.9 (0.5)	66.3 (0.3)	14.2 (0.5)	42.4 (0.004)	18.5 (0.6)	39.3 (0.1)	7.2 (0.2)	28.6 (0.1)	24.4 (0.5)	46.1 (0.2)
RG-I (mol%)	58.2 (1.6)	28.2 (0.5)	35.4 (0.3)	34.3 (0.04)	31.1 (0.2)	36.8 (0.1)	17.2 (0.04)	24.8 (0.1)	69.6 (0.5)	50.2 (0)
DM (%)	11 (5)	55 (0)	53 (0)	92 (0)	87 (0)	n.d.	40 (2)	n.d.	66 (18)	71 (1)
DA (%)	5 (1)	20 (0)	17 (0)	28 (0)	23 (0)	28 (1)	19 (2)	36 (0)	20 (1)	27 (2)

HG and RG-I contents (mol%) were calculated from the monosaccharide composition. Standard deviations are shown in parentheses based on two independent measurements. For further clarification of the abbreviations, see Fig. 1 and 2.

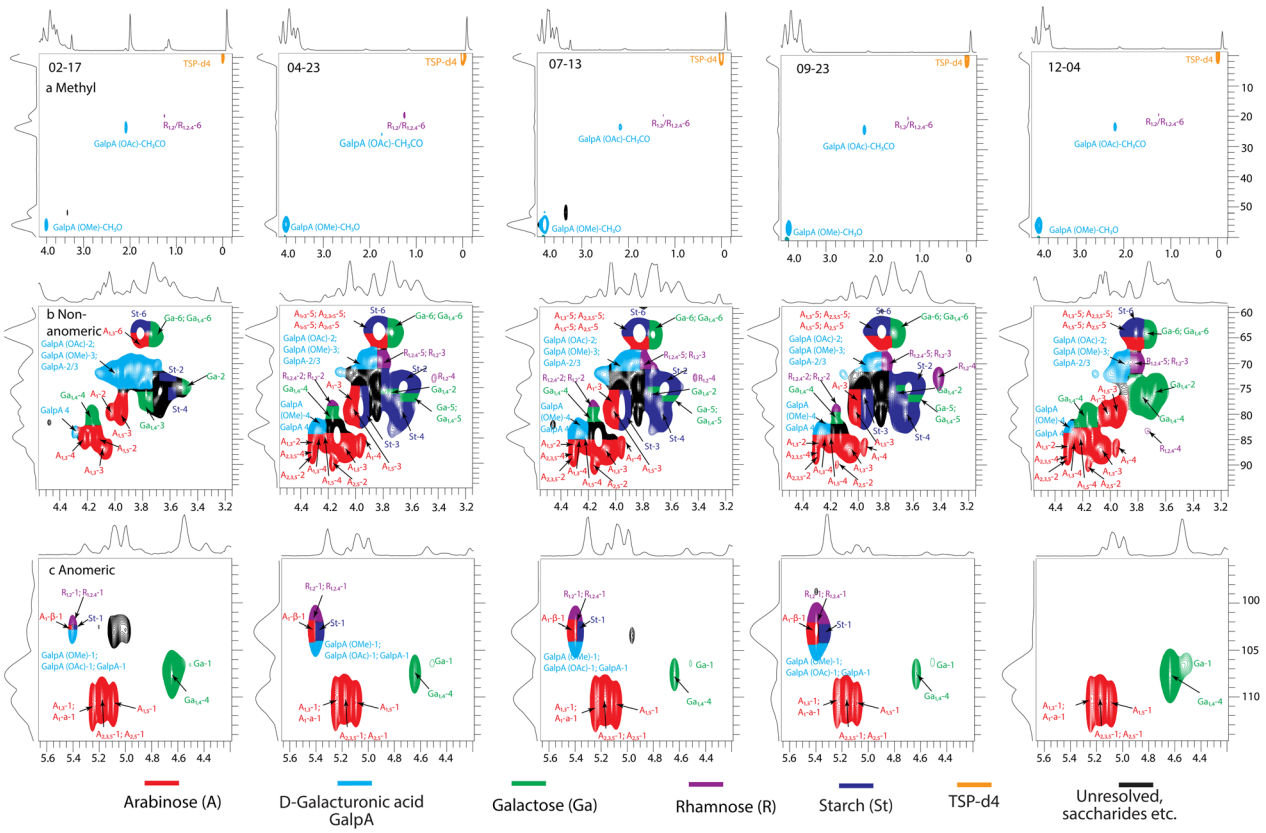

Fig. 3 2D heteronuclear single quantum coherence (HSQC) NMR spectrum of dialyzed citric acid extracted pectin (DCA-P) from five seasons of willow bark: 02-17; 04-23; 07-13; 09-23; 12-04. (a) Methyl (δ_C/δ_H, 0–59.84/0–3.943 ppm). (b) Non-anomeric methylene and methine (δ_C/δ_H, 58.82–94.67/3.155–4.548 ppm). (c) Anomeric methine group regions (δ_C/δ_H, 95.78–115/4.2–5.696 ppm). For abbreviations, see Fig. 1 and 2.

Table 2 Yield, weight-average molecular weight (M_w), dispersity (M_w/M_n), and chemical composition of purified hemicelluloses from five different samples: 02-17; 04-23; 07-13; 09-23; 12-04

	02-17	04-23	07-13	09-23	12-04
Yield (w/w% WB)	1 (0)	3 (0)	2 (0)	3 (0)	2 (0)
M_w (kDa)	29	35	44	32	33
M_w/M_n	1.4	1.5	1.6	1.5	1.5
Monosaccharides (mg g^{-1})					
Gal	48 (0)	29 (1)	28 (1)	28 (1)	37 (1)
Xyl	417 (2)	461 (6)	366 (1)	350 (0.4)	478 (0.4)
Characteristics					
Xylan-MG/xylan[a]	0.04 (0.01)	0.03 (0.01)	0.04 (0.02)	0.03 (0.02)	0.07 (0.002)
Degree of acetylation[b]	0.008	0.0001	0.006	0.004	0.005
Starch/xylan[c]	n.d.	0.006	0.02	0.01	n.d.

Standard deviations are shown in parentheses based on two independent measurements. For further clarification of the abbreviations, see Fig. 1. [a] Percentage ratio between volumes of xylan-MG and xylan (Xy-1 and Xy-4 for xylan; Xy-MG-1 and Xy-MG-4 for Xy-MG). [b] Percentage ratio between volumes of xylan-acetyl and xylan (Xy-5a for xylan; Xy-acetyl for acetylated xylan). [c] Percentage ratio between volumes of starch and xylan (Xy-4 for xylan; St-4 for starch).

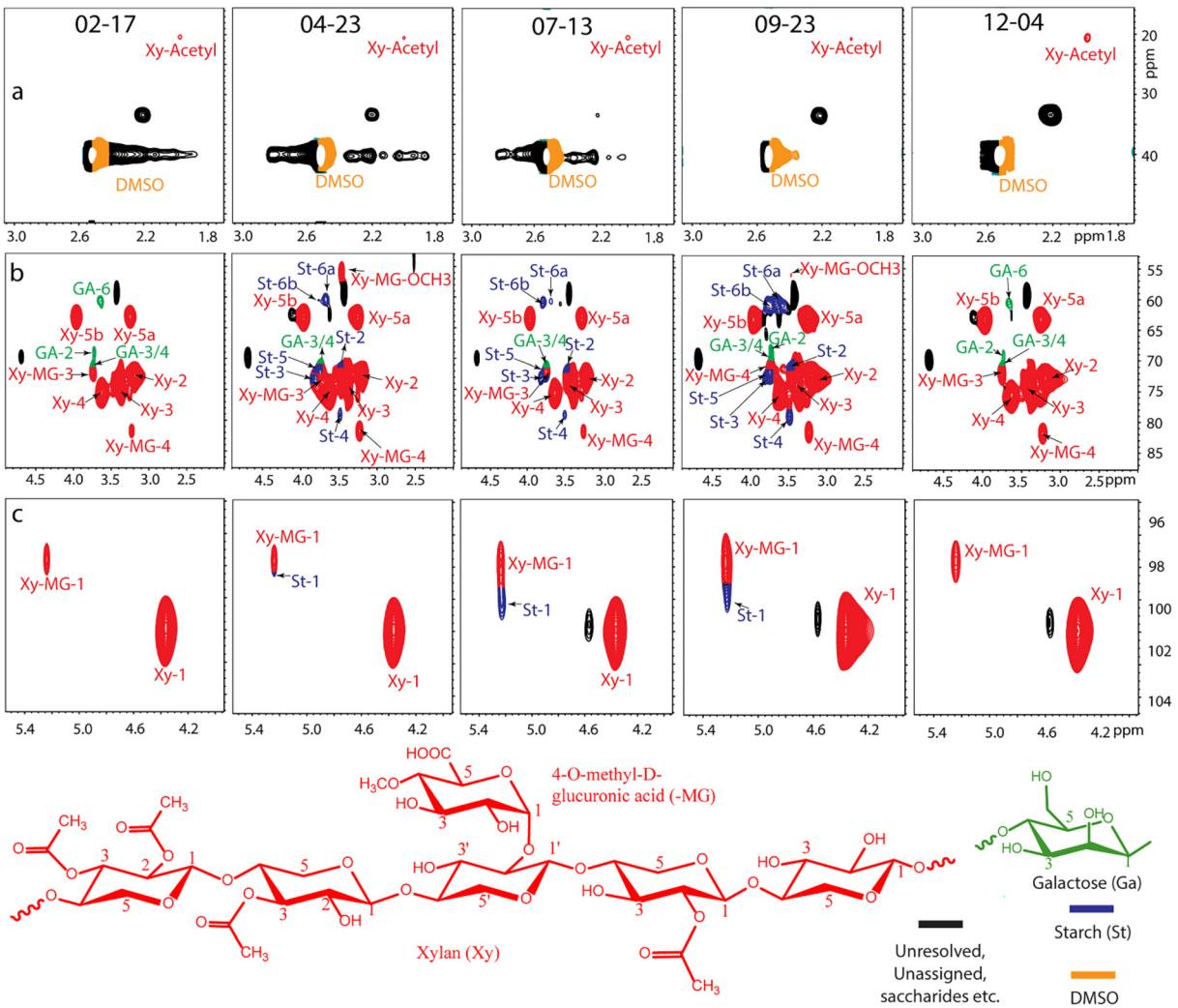

Fig. 4 2D HSQC NMR spectrum of hemicellulose fractions that are recovered from willow bark of different seasons: 02-17; 04-23; 07-13; 09-23; 12-04. (a) Methyl (δ_C/δ_H, 15.47–51.17/1.7–3.1 ppm). (b) Non-anomeric methylene and methine (δ_C/δ_H, 52.86–87.58/2.005–4.888 ppm). (c) Anomeric methine group regions (δ_C/δ_H, 93.88–106.96/3.943–5.538 ppm). For abbreviations, see Fig. 1.

consortium besides arabinose. In contrast, when the content of RG-I in pectin is low (*i.e.* 09-23), only the enzymes targeting the HG region need to be considered. The DM also influences the selection of HG-degrading enzymes. Pectate lyase and polygalacturonase show higher activity on low esterified pectin (*i.e.* 02-17), while pectin lyase and polymethyl galacturonase prefer highly esterified pectin (*i.e.* 07-13) with a high degree of esterification.[4,30,31] In addition, acetylated Gal*p*A residues can be removed by pectin/rhamnogalacturonan acetyl esterase. The correlation between the seasonal dynamics and the structure of pectin is reported for the first time, which provides the essential knowledge required for optimizing the microbial consortium in valorizing willow bark[4] that is harvested in multiple seasons.

Seasonal effect on hemicellulose

Pretreatment using citric acid is important not only for pectin chelation but also for removing metallic inorganic components, which is crucial for minimizing the reactivity of peracetic acid. The recovered hemicellulose yield is within the range of 1–3 wt% willow bark; nevertheless, this fraction of recovered hemicellulose may not represent all hemicelluloses. The molar mass distribution of cellulose shifted to a shoulder peak at lower molar mass (Fig. S4†), which indicates that the shoulder peaks can be attributed to unrecovered hemicelluloses.[32] Hemicelluloses from summer-harvested (07-13) pectin (>44 kDa) reached the maximum molecular mass that is recovered from other seasons (Table 2).

2D HSQC NMR (Fig. 4) has been applied to elucidate the linkage feature of hemicelluloses. The assignments were based on the references.[16,33,34] Willow bark's hemicellulose is not the same as xylan from a typical wood section of hardwood species, which contains very little (3–7%, Table 2) of the substituted –MG group. Specifically, C1/H1–C5/H5 of terminal xylose were identified for their characteristic peaks of 97.6/5.24, 72.7/3.19, 73.9/3.39, 75.5/3.62, and 63.2/3.25 (5a) and 3.96 (5b) ppm, respectively. The identified peak at δ_C/δ_H 20.4/1.97 ppm could be assigned to the acetyl group of xylan, although the degree of acetylation is less than 1% (Table 1). The peaks at δ_C/δ_H 81.7/3.23 (Xy-MG-4), δ_C/δ_H 72.1/3.74 (Xy-MG-3), and 97.6/5.24 ppm (Xy-MG-1) represent the C1/H1–C6/H6 correlations of the branched linkages between the 4-*O*-α-D-glucuronic acid (MeGlcA) and (1→4)-β-D-Xyl*p* ((1→4)-β-D-Xyl*p*-2-*O*-(4-OMe-D-Glc*p*A)), which were identified in all hemicellulose fractions (Fig. 4). δ_C/δ_H 55.9/3.46 (Xy-MG-OCH_3) is only identified for hemicellulose fractions of WB that is harvested at 04-23 and 09-23. Furthermore, a signal for starch was detected only in the hemicelluloses fractions (at 0.6–2% on the basis of xylan) from WB that is harvested from non-winter seasons (04-23, 07-13, and 09-23), indicating that DMSO is possibly capable of partially dissolving α-glucan starch besides hemicellulose.[35,36]

Seasonal effect on protein and starch through TG Raman spectroscopy

TG Raman spectroscopy has been implemented to analyze the bark non-destructively without any pretreatment and with a low fluorescence background. Therefore, prior to TG Raman acquisition (Fig. 5), individual spectra of the main components, including ferulic acid, starch, pectin, and lignin, were recorded with both TG and CW Raman (Fig. S5†). Generally, the typical fingerprint of polysaccharide spectra is represented by pectin, glucan, starch, protein, and glucuronoxylan (hemicellulose) that exhibit bands in these three domains based on the literature.[18,37–41] They could be assigned as C–O–C, C–O, and C–C stretching (1000–1200 cm^{-1}); CH/CH_2 deformation and C–O–H bending modes (1200–1500 cm^{-1}); and skeletal and torsional vibration modes (below 800 cm^{-1}). Interestingly, the peak intensity at 1440 cm^{-1} is assigned to a symmetric vibration of CH_2 stretching of lignin. The vibrational intensity of 1440 cm^{-1} has higher intensities for WB harvested in the winter season (12-04 and 02-17) than for WB that is harvested in other seasons, which is in line with the determined acid-insoluble lignin that is shown in Table S1.†

The vibration of starch was displayed at 478 cm^{-1} (skeletal vibration of the glucopyranose unit), 850/920 cm^{-1} (C–O–C), 1100 cm^{-1} (glycosidic link C–O–C), and 1372 cm^{-1} (C–O–H symmetric stretching of starch), as summarized in Table 3.[42] In particular, starch displayed a stronger band at 478 and 1378 cm^{-1} for bark that was harvested during non-winter seasons (04-23, 07-13, and 09-23), which supports the previous identifications that starch has a higher abundance in the recovered pectin and hemicellulose fractions. Moreover, the spectra show the characteristic signature of protein given by the amide I band (around 1650 cm^{-1}) that was assigned to the vibration of the *trans* peptide group C═ONH. Also, the amide III band (β-sheet) that arises from the combination of N–H bending and C–N stretching of the peptide group (1233 cm^{-1}), the sharp band of the phenylalanine ring vibration (1005 cm^{-1}), S–S carbohydrates (530–560 cm^{-1}), and aromatic amino acids (632 cm^{-1}). There are highly significant character-

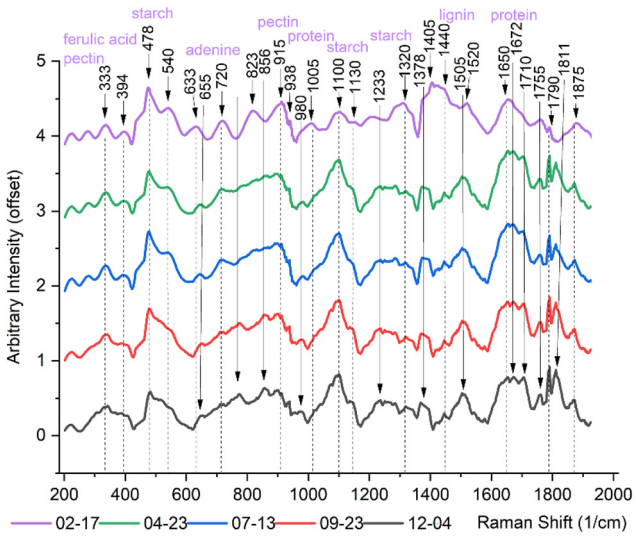

Fig. 5 Time-gated Raman spectroscopic analysis of willow bark that was harvested from 02-17 to 12-04 (Fig. 1). For assignments see Table 3.

Table 3 Tentative Raman band assignments based on literature and authentic compounds

Peaks [cm^{-1}]	Bond type/band assignment	Ref.[a]
333–394	Ferulic acid, pectin	45[a]
478	S–S stretch containing starch	42[a]
440	Pectin	[a]
530–560	S–S stretch, carbohydrates, proteins	18 and 37
632	C–C twist, aromatic amino acids	46
722	CH_2 rocking, nucleic acids (adenine)	47
823	C–O–C glycosidic link in RNA backbone	48
844/856	Pectin	49[a]
868/920	Starch	42
915	Pectin, cellulose	50[a]
938	Starch	42
980	Lignin	51
1005	CH_3 rocking of protein (phenylalanine)	47 and 52
1100	Carotenoids	52
1130	C–N stretch (starch)	52[a]
1165	Phenylalanine, tryptophan	38
1233	Amide III (β-sheet)	47
1320	C–C–C symmetric stretching, cellulose	52
1378	C–O–H symmetric stretching of starch	42
1405	Cellulose	51
1420–1450	Lignin $\upsilon(CH_2)$	51[a]
1520	C=C in the plane of carotenoids	52
1631	Lignin $\upsilon(CH_2)$ shoulder of 1600	51[a]
1650–1672	C=O stretch (amide I), protein	47

[a] The Raman spectrum of the authentic ferulic acid, starch, pectin, and lignin are summarized in Fig. S5.†

istic carbohydrate and protein peaks at 530–560 cm^{-1} as well as 632 and 1005 cm^{-1} for WB of 02-17 (late winter) and 12-04 (early winter) in comparison to other seasons. The parenchyma tissue from the inner bark might act as temporary storage of reduced nitrogen as a protein reserve in overwintering,[43] where the protein has previously been identified in the fraction of enzymatically purified lignin of willow bark.[44]

Conclusions

In this work, the chemical composition of willow bark has been demonstrated for its seasonal response to the harvesting seasons. Thus this information is interpreted in both a destructive manner (wet-chemical purification and characterization using NMR spectroscopy) and a non-destructive manner (novel time-gate Raman spectroscopy). The most striking seasonal effect involved the structural characteristics of pectin. Specifically, pectin showed clear structural differences as a response to the season, including the ratio and composition of HG and RG-I domains, and the branching profile of the RG-I sidechain. The correlation between seasonal dynamics and pectin structure is discussed for the first time, which provides the basic knowledge needed for optimizing the microbial consortium in valorizing willow bark that can possibly be harvested from multiple seasons. One of the major obstacles in further optimizing this "tailor-made enzyme consortium based on the structural features of the substrate" strategy[4] and "controlled valorization of willow bark as a source of biochemicals and fiber"[53] is simply the lack of a holistic approach to understand the seasonal effects on structural features of major constituents in the bark cell walls, namely pectin and hemicellulose. Pectinases and hemicellulases can then be tailored more precisely to liberate the sclerenchyma fiber bundle from the willow bark.

The identified starch in the recovered fractions of both pectin and hemicellulose was found to be more abundantly present in non-winter seasons (04-23, 07-13, and 09-23) than in winter seasons (02-17 and 12-04). This is also supported by the relatively higher abundance of starch in the native form of willow bark that is harvested in non-winter seasons, as revealed by Raman spectroscopy. Polarized Raman spectroscopy also revealed that protein is more pronounced at 02-17 (late winter) and 12-04 (early winter) in comparison to other seasons. In addition to the pectinases and hemicellulases, the addition of starch- and protein-degrading enzymes to the enzyme cocktail consortium might also be carefully tailored according to its season of harvesting. The synergetic (or competing) effects between different enzymes acting on substrates still need to be further optimized by response surface methodology (RSM) experiments and this will be systematically investigated in another study. TG Raman spectroscopy has not been implemented previously as a facile and non-destructive technique to reveal a structural profile from the original form of willow bark with a drastically reduced fluorescence background.

These findings remind us that we must carefully consider seasonal dynamics in tailoring the enzyme consortium to recover sclerenchyma fiber bundles from willow bark, which play a crucial role in further optimizing the "tailor-made enzyme consortium based on the structural features of the substrate" strategy.[4] It is also essential for designing controlled and tailored valorization strategies to utilize willow bark as a potential source of fiber bundles and extracts.[53] A similar strategy can be tailored for the valorization of bark from other fast-growing trees, such as eucalyptus and poplar. However, it is still far from an understanding of the specific mechanism involved in the regulation of all these structural fractions as a response to the season. The combination of classical wet-chemical characterization and non-destructive TG Raman paves the way for a more intuitive understanding of seasonal effects.

Conflicts of interest

The authors declare that they have no known competing financial interests.

Acknowledgements

This work also made use of the RawMatTERS Finland infrastructure (RAMI) facilities based at Aalto University. This work was a part of the Academy of Finland's Flagship Programme

under project no. 318890 and no. 318891 (Competence Center for Materials Bioeconomy, FinnCERES). VTT Finland was supported by the Academy of Finland, provided through an Academy of Finland Flagship Programme (PREIN) on Photonics Research and Innovation, PREIN, no. 320165. The authors thank the Sensing Solutions research area of VTT for their support with the spectroscopic equipment and measurement time.

References

1 M. K. Hassan, A. Villa, S. Kuittinen, J. Jänis and A. Pappinen, An assessment of side-stream generation from Finnish forest industry, *J. Mater. Cycles Waste Manage.*, 2019, **21**, 265–280, DOI: **10.1007/s10163-018-0787-5**.

2 E. Sjöstrom, *Wood Chemistry: Fundamentals and Applications*, Academic Press, New York, USA, 1981.

3 M. Lehr, M. Miltner and A. Friedl, Removal of wood extractives as pulp (pre-)treatment: a technological review, *SN Appl. Sci.*, 2021, **3**, 886, DOI: **10.1007/s42452-021-04873-1**.

4 J. Dou, J. Wang, J. Zhao and T. Vuorinen, Tailor-made enzyme consortium segregating sclerenchyma fibre bundles from willow bark, *Green Chem.*, 2022, **24**, 2576–2587, DOI: **10.1039/D2GC00188H**.

5 J. Dou, M. Rissanen, P. Ilina, H. Mäkkylä, P. Tammela, S. Haslinger and T. Vuorinen, Separation of fiber bundles from willow bark using sodium bicarbonate and their novel use in yarns for superior UV protection and antibacterial performance, *Ind. Crops Prod.*, 2021, **164**, 113387, DOI: **10.1016/j.indcrop.2021.113387**.

6 J. Dou, A. Karakoç, L. S. Johansson, S. Hietala, D. Evtyugin and T. Vuorinen, Mild alkaline separation of fiber bundles from eucalyptus bark and their composites with cellulose acetate butyrate, *Ind. Crops Prod.*, 2021, **165**, 113436, DOI: **10.1016/j.indcrop.2021.113436**.

7 S. Ö. Keleş, Variation in morphological and wood cell traits in coppice stems of *Populus nigra* L. and *Salix alba* L., *J. Forensic Sci.*, 2021, **67**, 396–407, DOI: **10.17221/208/2020-JFS**.

8 D. Mohnen, Pectin structure and biosynthesis, *Curr. Opin. Plant Biol.*, 2008, **11**, 266–277, DOI: **10.1016/j.pbi.2008.03.006**.

9 J. Harholt, A. Suttangkakul and H. V. Scheller, Biosynthesis of Pectin, *Plant Physiol.*, 2010, **153**, 384–395, DOI: **10.1104/pp.110.156588**.

10 T. Qu, R. Liu, W. Wang, L. An, T. Chen, G. Liu and Z. Zhao, Brassinosteroids regulate pectin methylesterase activity and *AtPME41* expression in *Arabidopsis* under chilling stress, *Cryobiology*, 2011, **63**, 111–117, DOI: **10.1016/j.cryobiol.2011.07.003**.

11 Y. Liu, H. Ahmad, Y. Luo, D. T. Gardiner, R. S. Gunasekera, W. L. McKeehan and B. S. Patil, Influence of harvest time on citrus pectin and its *in vitro* inhibition of fibroblast growth factor signal transduction, *J. Sci. Food Agric.*, 2002, **82**, 469–477, DOI: **10.1002/jsfa.1037**.

12 M. Baïer, R. Goldberg, A. M. Catesson, M. Liberman, N. Bouchemal, V. Michon and C. H. du Penhoat, Pectin changes in samples containing poplar cambium and inner bark in relation to the seasonal cycle, *Planta*, 1994, **193**, 446–454, DOI: **10.1007/BF00201825**.

13 E. N. Makarova, E. G. Shakhmatov and V. A. Belyy, Seasonal dynamics of polysaccharides in Norway spruce (*Picea abies*), *Carbohydr. Polym.*, 2017, **157**, 686–694, DOI: **10.1016/j.carbpol.2016.10.035**.

14 F. Dranca and M. Oroian, Extraction, purification and characterization of pectin from alternative sources with potential technological applications, *Food Res. Int.*, 2018, **113**, 327–350, DOI: **10.1016/j.foodres.2018.06.065**.

15 J. Berglund, D. Mikkelsen, B. M. Flanagan, S. Dhital, S. Gaunitz, G. Henriksson, M. E. Lindström, G. E. Yakubov, M. J. Gidley and F. Vilaplana, Wood hemicelluloses exert distinct biomechanical contributions to cellulose fibrillar networks, *Nat. Commun.*, 2020, **11**, 4692, DOI: **10.1038/s41467-020-18390-z**.

16 S. Sun, X. Cao, H. Li, F. Xu and R. Sun, Structural characterization of residual hemicelluloses from hydrothermal pretreated *Eucalyptus* fiber, *Int. J. Biol. Macromol.*, 2014, **69**, 158–164, DOI: **10.1016/j.ijbiomac.2014.05.037**.

17 D. V. Evtuguin, J. L. Tomás, A. M. S. Silva and C. P. Neto, Characterization of an acetylated heteroxylan from *Eucalyptus globulus* Labill, *Carbohydr. Res.*, 2003, **338**, 597–604, DOI: **10.1016/S0008-6215(02)00529-3**.

18 M. Kögler and B. Heilala, Time-gated Raman spectroscopy–a review, *Meas. Sci. Technol.*, 2020, **32**, 012002, DOI: **10.1088/1361-6501/abb044**.

19 A. Potthast, S. Radosta, B. Saake, S. Lebioda, T. Heinze, U. Henniges, A. Isogai, A. Koschella, P. Kosma, T. Rosenau, S. Schiehser, H. Sixta, M. Strlič, G. Strobin, W. Vorwerg and H. Wetzel, Comparison testing of methods for gel permeation chromatography of cellulose: coming closer to a standard protocol, *Cellulose*, 2015, **22**, 1591–1613, DOI: **10.1007/s10570-015-0586-2**.

20 J. Müller-Maatsch, A. Caligiani, T. Tedeschi, K. Elst and S. Sforza, Simple and Validated Quantitative ^{1}H NMR Method for the Determination of Methylation, Acetylation, and Feruloylation Degree of Pectin, *J. Agric. Food Chem.*, 2014, **62**, 9081–9087, DOI: **10.1021/jf502679s**.

21 E. N. Ashworth, V. E. Stirm and J. J. Volenec, Seasonal variations in soluble sugars and starch within woody stems of *Cornus sericea* L., *Tree Physiol.*, 1993, **13**, 379–388, DOI: **10.1093/treephys/13.4.379**.

22 J. J. Sauter and S. Wellenkamp, Seasonal Changes in Content of Starch, Protein and Sugars in the Twig Wood of *Salix caprea* L., *Holzforschung*, 1998, **52**, 255–262, DOI: **10.1515/hfsg.1998.52.3.255**.

23 C. Barbaroux and N. Bréda, Contrasting distribution and seasonal dynamics of carbohydrate reserves in stem wood of adult ring-porous sessile oak and diffuse-porous beech trees, *Tree Physiol.*, 2002, **22**, 1201–1210, DOI: **10.1093/treephys/22.17.1201**.

24 J. Dou, P. Ilina, J. Hemming, K. Malinen, H. Mäkkylä, N. O. de Farias, P. Tammela, G. D. A. Umbuzeiro,

R. Räisänen and T. Vuorinen, Effect of Hybrid Type and Harvesting Season on Phytochemistry and Antibacterial Activity of Extracted Metabolites from *Salix* Bark, *J. Agric. Food Chem.*, 2022, **70**, 2948–2956, DOI: 10.1021/acs.jafc.1c08161.

25 A. Janská, P. Maršík, S. Zelenková and J. Ovesná, Cold stress and acclimation – what is important for metabolic adjustment?, *Plant Biol.*, 2010, **12**, 395–405, DOI: 10.1111/j.1438-8677.2009.00299.x.

26 F. Kaplan, D. Y. Sung and C. L. Guy, Roles of β-amylase and starch breakdown during temperatures stress, *Physiol. Plant.*, 2006, **126**, 120–128, DOI: 10.1111/j.1399-3054.2006.00604.x.

27 J. J. Sauter and B. van Cleve, Storage, mobilization and interrelations of starch, sugars, protein and fat in the ray storage tissue of poplar trees, *Trees*, 1994, **8**, 297–304, DOI: 10.1007/BF00202674.

28 E. N. Makarova and E. G. Shakhmatov, Structural characteristics of oxalate-soluble polysaccharides from Norway spruce (*Picea abies*) foliage, *Carbohydr. Polym.*, 2020, **246**, 116544, DOI: 10.1016/j.carbpol.2020.116544.

29 E. G. Shakhmatov, P. V. Toukach, E. A. Michailowa and E. N. Makarova, Structural studies of arabinan-rich pectic polysaccharides from *Abies sibirica* L. Biological activity of pectins of *A. sibirica*, *Carbohydr. Polym.*, 2014, **113**, 515–524, DOI: 10.1016/j.carbpol.2014.07.037.

30 M. Zou, X. Li, J. Zhao and Y. Qu, Characteristics of Polygalacturonate Lyase C from *Bacillus subtilis* 7-3-3 and Its Synergistic Action with PelA in Enzymatic Degumming, *PLoS One*, 2013, **8**, e79357, DOI: 10.1371/journal.pone.0079357.

31 M. Zou, X. Li, W. Shi, F. Guo, J. Zhao and Y. Qu, Improved production of alkaline polygalacturonate lyase by homologous overexpression *pelA* in *Bacillus subtilis*, *Process Biochem.*, 2013, **48**, 1143–1150, DOI: 10.1016/j.procbio.2013.05.023.

32 T. Schult, T. Hjerde, O. I. Optun, P. J. Kleppe and S. Moe, Characterization of cellulose by SEC-MALLS, *Cellulose*, 2002, **9**, 149–158, DOI: 10.1023/A:1020139409903.

33 J. Ding, C. G. Yoo, Y. Pu, X. Meng, S. Bhagia, C. Yu and A. J. Ragauskas, Cellulolytic enzyme-aided extraction of hemicellulose from switchgrass and its characteristics, *Green Chem.*, 2019, **21**, 3902–3910, DOI: 10.1039/C9GC00252A.

34 T. Yuan, F. Xu, J. He and R. Sun, Structural and physicochemical characterization of hemicelluloses from ultrasound-assisted extractions of partially delignified fast-growing poplar wood through organic solvent and alkaline solutions, *Biotechnol. Adv.*, 2010, **28**, 583–593, DOI: 10.1016/j.biotechadv.2010.05.016.

35 S. Santacruz, K. Koch, R. Andersson and P. Åman, Characterization of Potato Leaf Starch, *J. Agric. Food Chem.*, 2004, **52**, 1985–1989, DOI: 10.1021/jf030601k.

36 D. S. Jackson, Solubility Behavior of Granular Corn Starches in Methyl Sulfoxide (DMSO) as Measured by High Performance Size Exclusion Chromatography, *Starch*, 1991, **43**, 422–427, DOI: 10.1002/star.19910431103.

37 A. Rygula, K. Majzner, K. M. Marzec, A. Kaczor, M. Pilarczyk and M. Baranska, Raman spectroscopy of proteins: a review, *J. Raman Spectrosc.*, 2013, **44**, 1061–1076, DOI: 10.1002/jrs.4335.

38 J. De Gelder, K. De Gussem, P. Vandenabeele and L. Moens, Reference database of Raman spectra of biological molecules, *J. Raman Spectrosc.*, 2007, **38**, 1133–1147, DOI: 10.1002/jrs.1734.

39 T. Rojalin, L. Kurki, T. Laaksonen, T. Viitala, J. Kostamovaara, K. C. Gordon, L. Galvis, S. Wachsmann-Hogiu, C. J. Strachan and M. Yliperttula, Fluorescence-suppressed time-resolved Raman spectroscopy of pharmaceuticals using complementary metal-oxide semiconductor (CMOS) single-photon avalanche diode (SPAD) detector, *Anal. Bioanal. Chem.*, 2016, **408**, 761–774, DOI: 10.1007/s00216-015-9156-6.

40 L. Galvis, C. G. Bertinetto, J. L. Putaux, N. Montesanti and T. Vuorinen, Crystallite orientation maps in starch granules from polarized Raman spectroscopy (PRS) data, *Carbohydr. Polym.*, 2016, **154**, 70–76, DOI: 10.1016/j.carbpol.2016.08.032.

41 J. Dou, W. Xu, J. J. Koivisto, J. K. Mobley, D. Padmakshan, M. Kögler, C. Xu, S. Willför, J. Ralph and T. Vuorinen, Characteristics of Hot Water Extracts from the Bark of Cultivated Willow (*Salix* sp.), *ACS Sustainable Chem. Eng.*, 2018, **6**, 5566–5573, DOI: 10.1021/acssuschemeng.8b00498.

42 Y. Liu, Y. Xu, Y. Yan, D. Hu, L. Yang and R. Shen, Application of Raman spectroscopy in structure analysis and crystallinity calculation of corn starch, *Starch*, 2015, **67**, 612–619, DOI: 10.1002/star.201400246.

43 J. S. Greenwood, C. Demmers and S. Wetzel, Seasonally dependent formation of protein-storage vacuoles in the inner bark tissues of tissues of *Salix microstachya*, *Can. J. Bot.*, 1990, **68**, 1747–1755, DOI: 10.1139/b90-225.

44 J. Dou, H. Kim, Y. Li, D. Padmakshan, F. Yue, J. Ralph and T. Vuorinen, Structural Characterization of Lignins from Willow Bark and Wood, *J. Agric. Food Chem.*, 2018, **66**, 7294–7300, DOI: 10.1021/acs.jafc.8b02014.

45 I. Aguilar-Hernández, N. K. Afseth, T. López-Luke, F. F. Contreras-Torres, J. P. Wold and N. Ornelas-Soto, Surface enhanced Raman spectroscopy of phenolic antioxidants: A systematic evaluation of ferulic acid, *p*-coumaric acid, caffeic acid and sinapic acid, *Vib. Spectrosc.*, 2017, **89**, 113–122, DOI: 10.1016/j.vibspec.2017.02.002.

46 E. Witkowska, T. Jagielski and A. Kamińska, Genus-and species-level identification of dermatophyte fungi by surface-enhanced Raman spectroscopy, *Spectrochim. Acta, Part A*, 2018, **192**, 285–290, DOI: 10.1016/j.saa.2017.11.008.

47 M. Kögler, J. Itkonen, T. Viitala and M. G. Casteleijn, Assessment of recombinant protein production in *E. coli* with Time-Gated Surface Enhanced Raman Spectroscopy (TG-SERS), *Sci. Rep.*, 2020, **10**, 2472, DOI: 10.1038/s41598-020-59091-3.

48 N. P. Ivleva, R. Niessner and U. Panne, Characterization and discrimination of pollen by Raman microscopy, *Anal. Bioanal. Chem.*, 2005, **381**, 261–267, DOI: 10.1007/s00216-004-2942-1.

49 H. Wu, H. Xu, H. Li, D. Wei, J. Lin and X. Li, Seasonal development of cambial activity in relation to xylem formation in Chinese fir, *J. Plant Physiol.*, 2016, **195**, 23–30, DOI: 10.1016/j.jplph.2015.12.013.

50 T. Dieing, O. Hollricher and J. Toporski, *Confocal Raman Microscopy*, Springer Berlin, Heidelberg, Germany, 2011. DOI: 10.1007/978-3-642-12522-5.

51 U. P. Agarwal, Analysis of cellulose and lignocellulose materials by Raman spectroscopy: a review of the current status, *Molecules*, 2019, **24**, 1659, DOI: 10.3390/molecules24091659.

52 W. Z. Payne and D. Kurouski, Raman spectroscopy enables phenotyping and assessment of nutrition values of plants: a review, *Plant Methods*, 2021, **17**, 78, DOI: 10.1186/s13007-021-00781-y.

53 J. Dou, L. Galvis, U. Holopainen-Mantila, M. Reza, T. Tamminen and T. Vuorinen, Morphology and Overall Chemical Characterization of Willow (Salix sp.) Inner Bark and Wood: Toward Controlled Deconstruction of Willow Biomass, *ACS Sustainable Chem. Eng.*, 2016, **4**, 3871–3876, DOI: 10.1021/acssuschemeng.6b00641.